International Journal of Solids and Structures 47 (2010) 1888–1898

Contents lists available at ScienceDirect

International Journal of Solids and Structures

journal homepage: www.elsevier.com/locate/ijsolstr

A Monte Carlo form-finding method for large scale regular and irregular tensegrity structures

Yue Li [a,b], Xi-Qiao Feng [a,*], Yan-Ping Cao [a], Huajian Gao [c]

[a] AML, Department of Engineering Mechanics, Tsinghua University, Beijing 100084, China
[b] Institute of Nuclear and New Energy Technology, Tsinghua University, Beijing 100084, China
[c] Division of Engineering, Brown University, Providence, RI 02912, USA

ARTICLE INFO

Article history:
Received 13 January 2009
Received in revised form 3 March 2010
Available online 31 March 2010

Keywords:
Tensegrity
Form-finding
Monte Carlo method

ABSTRACT

We propose a Monte Carlo form-finding method that employs a stochastic procedure to determine equilibrium configurations of a tensegrity structure. This method does not involve complicated matrix operations or symmetry analysis, works for arbitrary initial configurations, and can handle large scale regular or irregular tensegrity structures with or without material/geometrical constraints.

1. Introduction

Tensegrity structures are usually modeled as a set of discontinuous bars (or struts) and continuous strings (or cables) connected with frictionless ball joints. Both bars and strings are prestressed and subject to axial loads (Juan and Mirats Tur, 2008). The bars can bear both tensile and compressive forces, while the strings can withstand only tension. Many artificial and biological structures consisting of tensioned and compressed components can be considered as tensegrity. Over the last few decades, tensegrity structures have attracted considerable attention in a wide diversity of fields, e.g. architecture (Fu, 2005), mathematics (Connelly and Back, 1998), materials science (Luo et al., 2005), aerospace (Tibert and Pellegrino, 2002, 2003) and biology (Ingber, 1993, 1997; Pirentis and Lazopoulos, 2010).

The analysis and design of large-scale and complex tensegrity structures are distinctly different from those in classical structural mechanics. In the past decades, various methods have been proposed to design and optimize tensegrity structures with various topology and geometry (Snelson, 1965; Motro, 1984; Masic et al., 2005, 2006; Ehara and Kanno, 2010; Feng et al., in press; Li et al., 2010). All tensegrity structures are statically indeterminate (Calladine, 1978; Hanaor, 1988; Pellegrino and Calladine, 1986). After the topology of a tensegrity structure and the lengths of its elements have been specified, one needs to determine its self-equilibrated structural configuration, known as form-finding. Much effort has been directed towards tensegrity form-finding strategies; for state-of-the-art reviews, see e.g. Tibert and Pellegrino (2003), Juan and Mirats Tur (2008) and Sultan (2009). Analytical form-finding methods have been proposed for simple tensegrity structures with high symmetry (Connelly and Terrell, 1995; Vassart and Motro, 1999; Murakami and Nishimura, 2001; Sultan et al., 2001; Kenner, 2003), while numerical methods are usually necessary for general applications. Some of the existing methods are based on the concept of force density which is defined as the ratio between internal force and the associated element length (Linkwitz and Schek, 1971; Schek, 1974). By introducing force densities as auxiliary variables, the non-linear equilibrium equations become linear and the force densities in all elements can be determined for a pre-specified topology. Masic et al. (2005) integrated the force density method (Linkwitz and Schek, 1971; Vassart and Motro, 1999) with a non-linear optimization technique to find tensegrity structures under shape constraints. Zhang and Ohsaki (2005) and Estrada et al. (2006) developed a matrix iteration scheme to solve the force density equations for equilibrium configurations of structures with complex topology. Since the properties of the elements are usually not assigned a priori, the force density methods are regarded as "less than ideal for structures with some known, or desired element lengths" (Tibert and Pellegrino, 2003). Another class of form-finding methods is called dynamic relaxation which is essentially a pseudo-dynamical process in tensegrity form-finding. Motro (1984) and Zhang and Ohsaki (2006) used this method to find tensegrity structures with irregular topology and geometries. Dynamic relaxation methods treat tensegrity structures as a set of nodal masses and a set of elements with damping.

* Corresponding author. Tel.: +86 10 62772934; fax: +86 10 62781824.
E-mail address: fengxq@tsinghua.edu.cn (X.-Q. Feng).

0020-7683/$ - see front matter © 2010 Elsevier Ltd. All rights reserved.
doi:10.1016/j.ijsolstr.2010.03.026

Nomenclature

n_e	total number of elements
n_s	total number of strings
n_b	total number of bars
n_n	total number of nodes
l_0^i	original length of element i
k^i	stiffness of element i
z^i	element type. $z^i = 1$ for strings, and $z^i = 0$ for bars.
E^i	potential energy of element i
$\mathbf{t}^i$	internal force vector of element i
$\mathbf{g}^i$	coordinates vector of element i
l^i	length of element i, defined as $l^i = \|\mathbf{g}^i\|$
$\mathbf{p}^j$	coordinates vector of node j
$\mathbf{f}^j$	external force vector on node j
$\mathbf{C}$	connectivity matrix
u^j	number of nodes that connects with the node j
$\mathbf{M}^j$	list of elements that contain the node j
$\mathbf{N}^j$	list of nodes that connect with the node j
$\mathbf{O}^j$	direction list of the elements in $\mathbf{M}^j$
I	superscript i stands for the parameters of the ith element, with $i = 1,2,\ldots,n_e$
j, k	superscript j (or k) stands for the parameters of the jth (or kth) node, with $j,k = 1,2, \ldots,n_n$

In each iteration step of dynamics relaxation, all nodes are moved simultaneously with velocities calculated from nodal forces. In such methods, the solution may oscillate around some particular states of a structure. Consequently, dynamic relaxation methods can become ineffective for large scale tensegrity structures (Tibert and Pellegrino, 2003). Recently, Rieffel et al. (2009) utilized an evolutionary algorithm to generate tensegrity structures and then reproduced the configurations via a rigid body dynamics simulation technique similar to the dynamics relaxation method. Pagitz and Mirats Tur (2009) proposed a form-finding algorithm for tensegrity structures which is based on the finite element method. A number of other form-finding methods have also been suggested in the literature, e.g. the genetic algorithm (Paul et al., 2005).

In spite of the above developments, however, there is still a demand to establish more versatile and robust methods to find tensegrity structural forms of relatively large scales or with irregular and unsymmetrical geometries. To this end, we propose a novel method by incorporating a Monte Carlo type approach into tensegrity form-finding. The Monte Carlo method, coined by Metropolis and Ulam (1949), was initially introduced to simulate a stochastic process by generating random moves that are either accepted or rejected according to a given probability distribution function. The proposed Monte Carlo form-finding (MCFF) method does not involve complicated matrix manipulations and is enhanced with a number of special techniques to accelerate convergence. In this study, all the bars and strings are assumed to be elastic and connected via frictionless ball joints (Tibert and Pellegrino, 2003). The influences of such factors as gravity and damping on the final equilibrium configuration are neglected. It will be demonstrated that this method can solve large scale form-finding problems for both regular and irregular tensegrity structures.

The outline of this paper is as follows. In Section 2, we will describe the basic idea and procedure of the proposed Monte Carlo method for tensegrity form-finding. In Section 3, the detailed process of numerical implementation and enhancement techniques to improve the speed of convergence will be discussed. Several examples are given in Section 4 to illustrate the efficacy of the proposed form-finding method.

2. Monte Carlo form-finding method

Stochastic search and optimization methods have seen substantial progresses in recent decades; for state-of-the-art review, see Spall (2003). In particular, the Monte Carlo method is now widely used in a variety of mathematical and physical sciences, especially in molecular simulations. The Monte Carlo method used in most molecular simulations is based on an accept-or-reject scheme (Metropolis et al., 1953). In each step, one generates a trial configuration through random sampling, which is then compared with the configuration of the previous step. If the trial configuration has lower energy than the previous one, it will be accepted; otherwise it has a finite probability of being rejected. In the present paper, the conventional Monte Carlo method will be modified to solve tensegrity form-finding problems. The nodes and elements of a tensegrity are considered as atoms and atomic bonds, respectively. In this sense, a tensegrity structure is just like a molecule, and the tensegrity form-finding resembles a process of molecular relaxation. Based on this idea, we develop a Monte Carlo form-finding (MCFF) procedure that includes the following steps.

Initialization:

(1) Specify the basic information of the structure, select a random configuration as the initial configuration P_0, and set the iteration step as $n = 1$.
(2) For each node j and element i, compute the neighbor lists $\mathbf{M}^j$, $\mathbf{N}^j$, $\mathbf{O}^j$, the internal force vector $\mathbf{t}^i$, the resultant nodal force vector $\mathbf{f}^j$, the element potential energy E^i, the total energy E_0, and other parameters. The definitions of these parameters will be given in Section 3.

Iterations:

(3) Select a random node and give this node a random displacement to generate a trial configuration P_t.
(4) Compare the potential energy E of the trial configuration P_t with that of the previous step P_{n-1}. If the energy decreases, the trial configuration will be accepted as the configuration for the next iteration step, i.e., $P_n = P_t$. Otherwise, the trial configuration will be rejected and the configuration will remain the same as the previous one, i.e. $P_n = P_{n-1}$.
(5) If the system is not in equilibrium, set $n = n + 1$ and go to step 3.

Termination:

(6) When the equilibrium state is reached, the iteration will be terminated, and the final configuration is thought as a stable form of tensegrity.

It should be pointed out that, although the present tensegrity form-finding method is inspired by the Monte Carlo method for molecular simulations, there are significant differences between the two. In molecular simulations, the final state of the system is

in detailed balance (Kalos and Whitlock, 1986) and the system energy obeys the Maxwell–Boltzmann distribution. If the trial configuration has energy lower than the previous one, it will be accepted; otherwise a random number $\xi \in (0,1)$ is generated and the trial configuration is accepted only if $\xi \leqslant \exp(-\Delta E/kT)$ (Metropolis et al., 1953), where ΔE is the energy change, T the absolute temperature, and k the Boltzmann constant. In contrast, the equilibrium state of a tensegrity structure is deterministic and temperature is of no relevance in the form-finding process. In the MCFF procedure, the resultant force on each node $\|\mathbf{f}_i\|$ is calculated and used as a criterion to judge whether equilibrium has been reached or not. In practice, only one node is moved in each iteration step so that only a small fraction of nodal forces need to be updated; see further discussions following Eqs. (17) and (18). A random trial configuration is accepted or rejected solely based on the sign of the energy change ΔE between the trial and the previous configurations. In addition, MCFF calculations are normally easier to perform than Monte Carlo molecular simulations in the following aspects. First, in contrast to molecular simulations, the neighbors of each node do not change in the form-finding process for a specified topology of tensegrity. Second, the force between two connected nodes is only a function of their distance, resembling a pair potential instead of more complicated many-body potentials used in most molecular simulations. These features of the MCFF method can greatly reduce the cost associated with the update of neighbor lists and the calculation of system energy.

We also note that our MCFF procedure shares several features in common with other form-finding methods. First, the essence of the MCFF procedure is to search for the equilibrium state of a tensegrity structure corresponding to a local minimum of system energy. A similar idea was used by Connelly (1993) to seek local energy minimum by testing whether the stress matrix is positive semi-definite. The Monte Carlo form-finding process allows us to solve more complex, large scale problems. Second, similar to the dynamic relaxation method, the MCFF procedure is also a pseudo dynamic process. In the MCFF procedure, only those trial configurations that lower the system energy will be accepted in the iteration procedure, which is definitely achievable by moving one of nodes appropriately.

3. Numerical implementation

The numerical implementation of the MCFF procedure consists of the six main steps described in Section 2. In what follows, we discuss some details of the implementation and a number of special techniques that can be applied to accelerate the convergence of the algorithm.

3.1. Input parameters

Before computation, an input file is prepared which contains the following information:

i. *Basic information of the model*: the total number of bars, strings, elements, and nodes, which are denoted as n_b, n_s, n_e, and n_n, respectively.
ii. *Required precision:* the maximum error ε that can be tolerated in judging if the system has reached equilibrium. The definition of ε will be given in detail in Section 3.5.
iii. *Topology information:* connectivity matrix **C**, i.e. the node numbers of each element and the element type z^i. We define $z^i = 1$ if the element is a string, and $z^i = 0$ if it is a bar.
iv. *Properties of elements:* the original (resting) lengths l_0^i $(i = 1, 2, \ldots, n_e)$, and the relationship between the internal force and the length change of each element.
v. *Initial nodal coordinates:* In this step, the initial nodal coordinates $\mathbf{P}_0^j$ can be set by selecting a random configuration. The MCFF procedure can be used to solve a form-finding problem without any prior knowledge of the final configuration. On the other hand, faster convergence can be expected if $\mathbf{p}_0^j$ is selected to be near equilibrium.

3.2. Other parameters used in the iteration

After the input file is established, the next step is to compute several system parameters. Some parameters are constant in the whole form-finding process, such as the neighbor lists, while others (e.g., the internal force of elements and the nodal force) are updated in each iteration step.

Neighbor lists: In the previous literature (e.g., Williamson et al., 2003), the topology of tensegrity is often described by an oriented graph, which can be denoted by a connectivity matrix $\mathbf{C} \in R^{e\times 2}$. In our iteration procedure, however, we use the neighbor lists, instead of **C**, to describe the relations between elements in the structure. By this approach, no complicated matrix manipulation is needed. We let the column vector $\mathbf{N}^j$ denote the neighbor list of all nodes that connect with the jth node, $\mathbf{M}^j$ the list of all elements that contain the jth node, $\mathbf{O}^j$ and the list of directions of the elements in $\mathbf{M}^j$. The direction of an element in $\mathbf{O}^j$ is represented as if the element vector enters, and 1 if it leaves the jth node. It is noted that the neighbor lists of all nodes can be obtained easily by a simple sequential traversal of the connectivity matrix **C**.

The pseudo code of this process is shown in Fig. 1, where the superscripts and subscripts indicate the rows and columns of a matrix, respectively; $\boldsymbol{u}$ is a column vector, with its jth row u^j containing the number of nodes connecting with the jth node. For the jth node shown in Fig. 2, for example, u^j equals 3 and its neighbor lists are $\boldsymbol{M}^j = [i_1, i_2, i_3]$, $\mathbf{N}^j = [j_1, j_2, j_3]$, and $\boldsymbol{O}^j = [1, -1, 1]$.

$i = 1;\ \boldsymbol{u} = \boldsymbol{0}\ (\boldsymbol{u} \in R^{n_e})$
when $i \le n_e$ do
  $j = C_1^i,\ k = C_2^i$
  $u^j = u^j + 1,\ u^k = u^k + 1;$
  $M_{u^j}^j = i,\ M_{u^k}^k = i;$
  $N_{u^j}^j = k,\ N_{u^k}^k = j;$
  $O_{u^j}^j = 1,\ O_{u^k}^k = -1;$
  $i = i + 1$
end

Fig. 1. A pseudo code to calculate the neighbor lists of nodes.

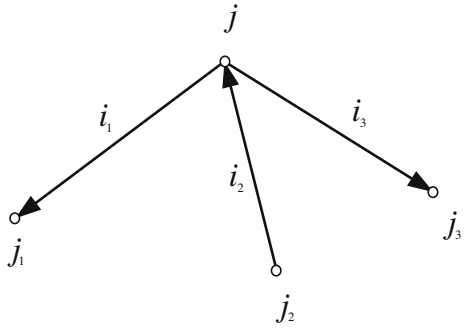

Fig. 2. Schematic diagram of an example to show the neighbors of the node j.

Length of elements: For element i, with the direction from node j to k, its element vector is defined as

$$\mathbf{g}^i = \mathbf{p}^k - \mathbf{p}^j, \tag{1}$$

and its current length is

$$l^i = \|\mathbf{g}^i\| = \sqrt{(x^j - x^k)^2 + (y^j - y^k)^2 + (z^j - z^k)^2}. \tag{2}$$

Internal forces: The internal force of elastic element i can be related to its elongation $\Delta l^i = (l^i - l_0^i)$ as

$$t^i = F(\Delta l^i) = F(l^i - l_0^i). \tag{3}$$

In the present paper, we assume all elements are linear elastic. Considering the fact that a string cannot bear a compressive force, Eq. (3) becomes

$$t^i = \begin{cases} 0 & \text{for a string element } (z^i = 1) \text{ with } l^i \leqslant l_0^i, \\ k^i(l^i - l_0^i) & \text{otherwise}, \end{cases} \tag{4}$$

where k^i denotes the stiffness of element i. Eq. (4) implies that the strings are allowed to be slack during iteration. However, if a string is slack in the final equilibrium configuration, it will be eliminable. In practical design, the slacking of strings seldom happens except when the specified topology has too many redundant strings or the resting lengths of some strings are too long. Since the internal force of an element is always along its axial direction, the internal force vector $\mathbf{t}^i$ is defined to have the same direction as $\mathbf{g}^i$, i.e.

$$\mathbf{t}^i = t^i \frac{\mathbf{g}^i}{\|\mathbf{g}^i\|}. \tag{5}$$

Resultant nodal forces: The resultant force $\mathbf{f}^j$ on node j can be obtained from internal force vectors in the elements connecting with this node. Considering the directions of $\mathbf{g}$ and $\mathbf{t}$ defined in Eqs. (1) and (5) as well as the definition of the neighbor element direction, the resultant force $\mathbf{f}^j$ is determined from

$$\mathbf{f}^j = \sum_{m=1}^{u^j} O_m^j \mathbf{t}^{N_m^j}. \tag{6}$$

Elastic potential energy: The elastic potential energy E^i of the element i is calculated by the following integral

$$E^i = \int_0^{l^i - l_0^i} F(l^i - l_0^i)\mathrm{d}(l^i - l_0^i). \tag{7}$$

For a linear elastic element, Eq. (7) reduces to

$$E^i = \begin{cases} 0 & \text{for a string element } (z^i = 1) \text{ with } l^i \leqslant l_0^i, \\ \frac{1}{2}k^i(l^i - l_0^i)^2 & \text{otherwise} \end{cases}. \tag{8}$$

The total energy of the structure is then

$$E = \sum_{i=1}^{n_e} E^i. \tag{9}$$

Eqs. (1)–(9) define all the parameters to be used in our calculation.

3.3. Selection of trial configurations

Before each iteration step, we specify a trial configuration by choosing a random node and giving this node a random displacement.

In the selection of the random node, one may simply assume that all nodes have the same probability to be selected, but this may lead to very slow convergence. If some nodes in the tensegrity structure have already approached their equilibrium positions, moving these nodes would not help convergence. In our calculations, therefore, we try to assign those far-from-equilibrium nodes higher probabilities to be selected than the near-equilibrium ones. Specifically, for each node j, we generate a random number η^j with uniform distribution on the interval (0,1) and multiply this number with the resultant nodal force f^j. The node with the maximum weighted product $\eta^j f^j$ will be selected, and a random displacement $\Delta\mathbf{p}^j$ is given to this node.

The trial displacement vector $\Delta\mathbf{p}^j$ also has a significant influence on the convergence speed. We specify $\Delta\mathbf{p}^j$ based on the following analysis aimed to create a trial displacement vector $\Delta\mathbf{p}^j$ for quick convergence. For cylindrical, spherical and some other types of tensegrity structures with all elements having the same stiffness k, a large number of tests have been conducted by assuming different trial displacements. Fig. 3 shows the distributions of the accepted displacements (solid blue diamonds) and the rejected displacements (empty red squares), according to the scheme described in the next subsection, in a polar coordinate system, where the normalized displacement $\|\Delta\mathbf{p}^j\|k/f^j$ is used as the radial coordinate and the angle $\phi(0 \leqslant \phi \leqslant \pi)$ between the nodal force and the nodal displacement as the angular coordinate. This figure shows that the displacement magnitude $\|\Delta\mathbf{p}^j\|$ has a significant impact on the convergence speed. If $\|\Delta\mathbf{p}^j\|$ is too large, the selected trial displacement $\Delta\mathbf{p}^j$ will be rejected in a majority of cases, causing a waste of computational time. On the other hand, a very small magnitude of $\Delta\mathbf{p}^j$ leads to insignificant configuration changes in each iteration step, even though $\Delta\mathbf{p}^j$ is acceptable. Fig. 3 also

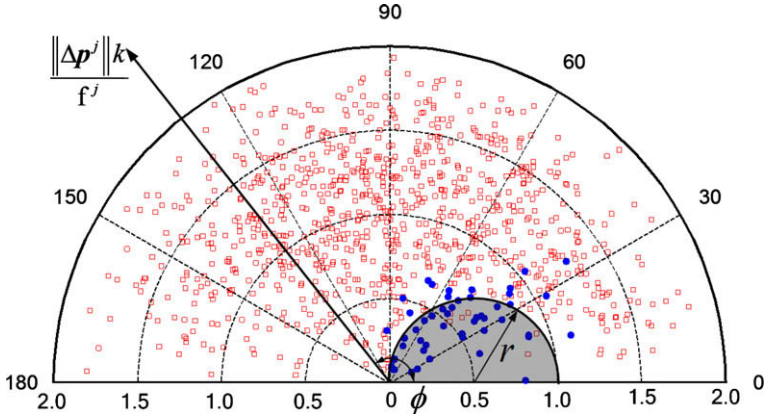

Fig. 3. Tested cases showing the statistics of accepted or rejected trial displacements Δp^j. The solid blue diamonds stand for the accepted trial displacements, and empty red squares those rejected. (For interpretation of references to color, the reader is referred to the web version of this article.)

indicates that the direction of $\Delta\mathbf{p}^j$ has a significant impact on convergence. Almost all $\Delta\mathbf{p}^j$ selections at an obtuse angle with respect to $\mathbf{f}^j$ are rejected. According to the above analysis, we suggest selecting the random displacement only in the sphere represented by the grey half circle with a radius of $r = 0.5$.

If a structure in design is to have some fixed nodes (i.e., geometrical constraints), rigid bars or inextensible strings, the trial configurations should be constrained correspondingly. None of the fixed nodes should be allowed to move in each iteration step and the associated nodal force will not be included in the computation of error. For rigid bars, the bar lengths are prescribed so that one node of an element is constrained on a spherical surface centered at the other node of the same element. Since a rigid bar can balance any load along its length direction, only the transverse component of a nodal force will be considered and the nodal displacement is limited on a surface. In this way, the number of degrees of freedom is reduced, leading to faster convergence. Inextensible string elements can be treated in a similar manner.

In addition, it is worth pointing out that the stiffness ratio between bars and strings can also influence the convergence speed. Fastest convergence is found when the stiffness ratio is near 1. Although the above analysis was conducted for the case where all elements have the same stiffness, the scheme is expected to work for more general cases.

3.4. Accept/reject scheme

In this subsection, we will describe the criterion for determining whether a random displacement should be accepted or rejected. After creating a random displacement $\Delta\mathbf{p}^j$ for node j, this node is moved to a new position

$$\bar{\mathbf{p}}^j = \mathbf{p}^j + \Delta\mathbf{p}^j, \tag{10}$$

where the overbar stands for quantities associated with a trial configuration. Assuming that the positions of all other nodes do not change, only the length vectors of those elements containing node j need to be updated. The new length vectors of these elements are

$$\bar{\mathbf{g}}^{M^j_m} = O^j_m(\bar{\mathbf{p}}^j - \mathbf{p}^{N^j_m}) \quad m = 1, 2, \ldots, u^j. \tag{11}$$

From Eqs. (2), (4) and (8), one can determine the element lengths, internal forces, and elastic energies corresponding to the trial configuration as

$$\bar{l}^i = \|\mathbf{g}^i\|, \tag{12}$$

$$\bar{t}^i = k^i(\bar{l}^i - l^i_0), \tag{13}$$

$$\bar{E}^i = \frac{1}{2}\bar{t}^i(\bar{l}^i - l^i_0), \tag{14}$$

respectively, where $i \in \mathbf{M}^j$.

According to the principle of minimum potential energy, the MCFF method adopts an accept/reject criterion based on change in system energy, which is similar to that used in molecular simulations. It is worth mentioning that only a few elements are involved in computing the change in system energy

$$\Delta E = \sum_{i\in\mathbf{M}^j}(\bar{E}^i - E^i). \tag{15}$$

In our scheme, a random movement is accepted only when the total potential energy does not increase, i.e.

$$\Delta E \leqslant 0. \tag{16}$$

Otherwise, the move is rejected, and we repeat the above procedure with a new trial configuration obtained according to Section 3.3.

If the trial configuration is accepted, the length vectors, the element lengths, the magnitudes of the internal forces, and the elastic strain energies of the u^j neighbor elements of the selected node j are updated using Eqs. (11)–(14). From Eq. (5), the element internal force vectors are

$$\bar{\mathbf{t}}^i = \bar{t}^i\frac{\bar{\mathbf{g}}^i}{\bar{l}^i} \quad (i \in \mathbf{M}^j). \tag{17}$$

Due to the change of internal forces in all elements connecting with the node j, the nodal force $\mathbf{f}^j$ is be updated by Eq. (6), and forces on the neighboring nodes of j change according to

$$\bar{\mathbf{f}}^{N^j_m} = \mathbf{f}^{N^j_m} + O^j_m(\bar{\mathbf{t}}^{M^j_m} - \mathbf{t}^{M^j_m}) \quad (m = 1, 2, \ldots, u^j). \tag{18}$$

The updated $\mathbf{g}^i$, l^i, t^i, E^i and $\mathbf{f}^k (i \in \mathbf{M}^j, k \in \mathbf{N}^j)$ are used in the next iteration step of the form-finding procedure. It can be seen from Eqs. (17) and (18) that only resultant forces on the selected node j and its u^j neighbor nodes need to be updated in each iteration step. For most tensegrity structures, u^j is generally in the range from 3 to 5, and the present method is much faster than methods that update all nodal forces in each step.

Since the form-finding process is aimed to search for the structural configuration with minimum potential energy $E_{\min}$, it can also be formulated as the following optimization problem:

$$E_{\min} = \min\sum_{i=1}^{n_e} E^i(\mathbf{p}), \tag{19}$$

where the elastic strain energy of the i-th element is calculated by

$$E^i = \begin{cases} 0, & \text{for a slack string;} \\ \text{constant}, & \text{for a rigid bar or an inextensible string;} \\ \frac{1}{2}k_i\left(\sqrt{(x^{C^i_1} - x^{C^i_2}) + (y^{C^i_1} - y^{C^i_2}) + (z^{C^i_1} - z^{C^i_2})} - l^i_0\right)^2, & \\ & \text{otherwise.} \end{cases} \tag{20}$$

Our calculations demonstrate that the Monte Carlo method can solve such a complicated non-linear optimization problem, even for large and irregular structures, as will be shown in Section 4.

3.5. Termination criterion

Theoretically, all nodes in a tensegrity should be in equilibrium at the final stage of the form-finding process. In other words, the resultant forces on all nodes vanish at equilibrium, i.e.,

$$\|\mathbf{f}^j\| = 0 \quad (j = 1, 2, \ldots, n_n). \tag{21}$$

In our numerical procedure, we set an error of tolerance ϵ to judge whether the system has reached equilibrium. The error from equilibrium is defined as the maximum nodal force, that is,

$$\text{error} = \max_{j=1,2,\ldots,n_n}\|\mathbf{f}^j\|. \tag{22}$$

The iteration is terminated once the following criterion is satisfied,

$$\text{error} \leqslant \varepsilon, \tag{23}$$

and the corresponding structure is regarded as an equilibrium form of tensegrity. The MCFF method is aimed to find an equilibrium configuration of local energy minimum. Each step of iteration is a perturbation of the system. After the criterion in Eq. (23) has been satisfied, a sufficient number (e.g., $10^4 \times n_n$) of iterations are performed further to check whether the calculated structure is stable.

Finally, the calculated structure is recorded in an output file, including the topology information (e.g., the connectivity matrix

with neighbor lists), the geometry information (e.g., coordinates of nodes, lengths and length vectors of elements), and the mechanical information (e.g., internal forces of elements and the total energy) of the structure.

4. Examples

In this section, we demonstrate the efficacy of the proposed MCFF method with a number of illustrative examples of tensegrity form-finding.

4.1. Cylindrical tensegrity structures

We first consider the well-known example of cylindrical tensegrities, also referred to as tensegrity prisms. Such a structure has two parallel regular polygons on both top and bottom, each consisting of v nodes v and strings. The two polygons are connected into a tensegrity prism by v bars and v strings. Fig. 4 illustrates the elements connected to node 1 on the bottom polygon, where a is an integer smaller than v, and θ is the relative twist angle between the top and bottom polygons. The analytical solution of the form-finding of such a tensegrity structure is (Connelly and Terrell, 1995)

$$\theta = \pi\left(\frac{1}{2} - \frac{a}{v}\right). \tag{24}$$

For the cylindrical tensegrity, we assume all bars have the same length. The strings on the cylindrical surface are a little shorter than the bars, and the length of the strings on top and bottom surfaces are determined according to the approximate ratio between the height and the radius of the cylinder. After properly setting the original length of elements, we can use the MCFF procedure to determine the equilibrium configuration of a cylindrical tensegrity. For instance, the results of triplex and pentaplex tensegrity with $a = 1$ are shown in Fig. 5(a) and (b), respectively. More complex cylindrical tensegrities are shown in Fig. 5(c)–(e), corresponding to the cases of $(v = 20, a = 2)$, $(v = 50, a = 10)$, and $(v = 100, a = 30)$, respectively. A larger scale sample with $v = 2000$ and $a = 1$ can be found in Fig. 5(f).

The accuracy of the MCFF procedure is demonstrated by comparing the numerical results with the analytical solution in Eq. (24). The relationship between θ and v is shown in Fig. 6 for various values of v and a, where the analytical solutions shown in curves are in excellent agreement with the calculated results from the MCFF method shown in solid circles.

As a more complicated type of cylindrical tensegrity, multistage tensegrity towers (Murakami and Nishimura, 2001) are calculated by the MCFF method. Fig. 7 shows the form-finding result of a 20 stage tower, each stage having 6 bars.

The calculation speed of the MCFF method is tested on a PC with only one Intel P4 2.8c processor and GFortran 4.1 complier. Since

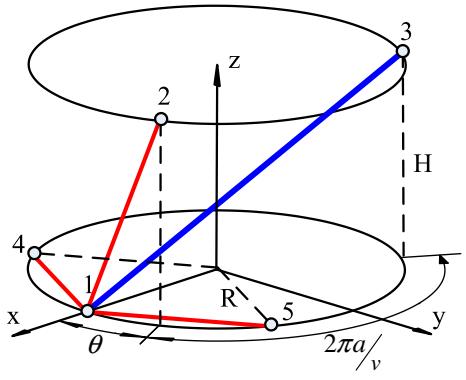

Fig. 4. The elements adjacent to node 1 in a tensegrity cylinder.

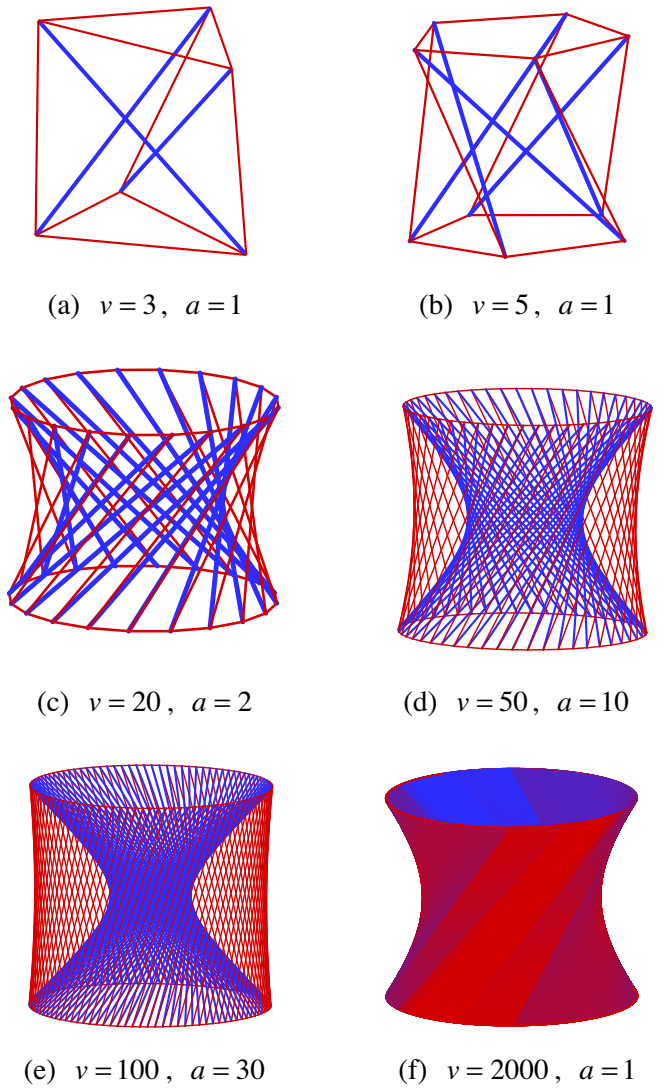

Fig. 5. The forms of cylindrical tensegrity structures found by the MCFF method.

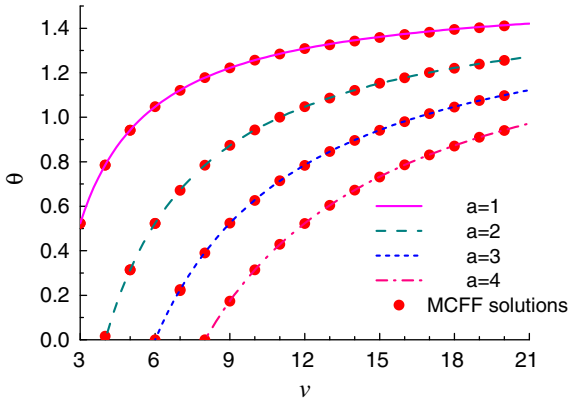

Fig. 6. Comparison of the analytical solutions (curves) and the MCFF results (solid circles) on the relationship between θ and v, when $a = 1,2,3,4$.

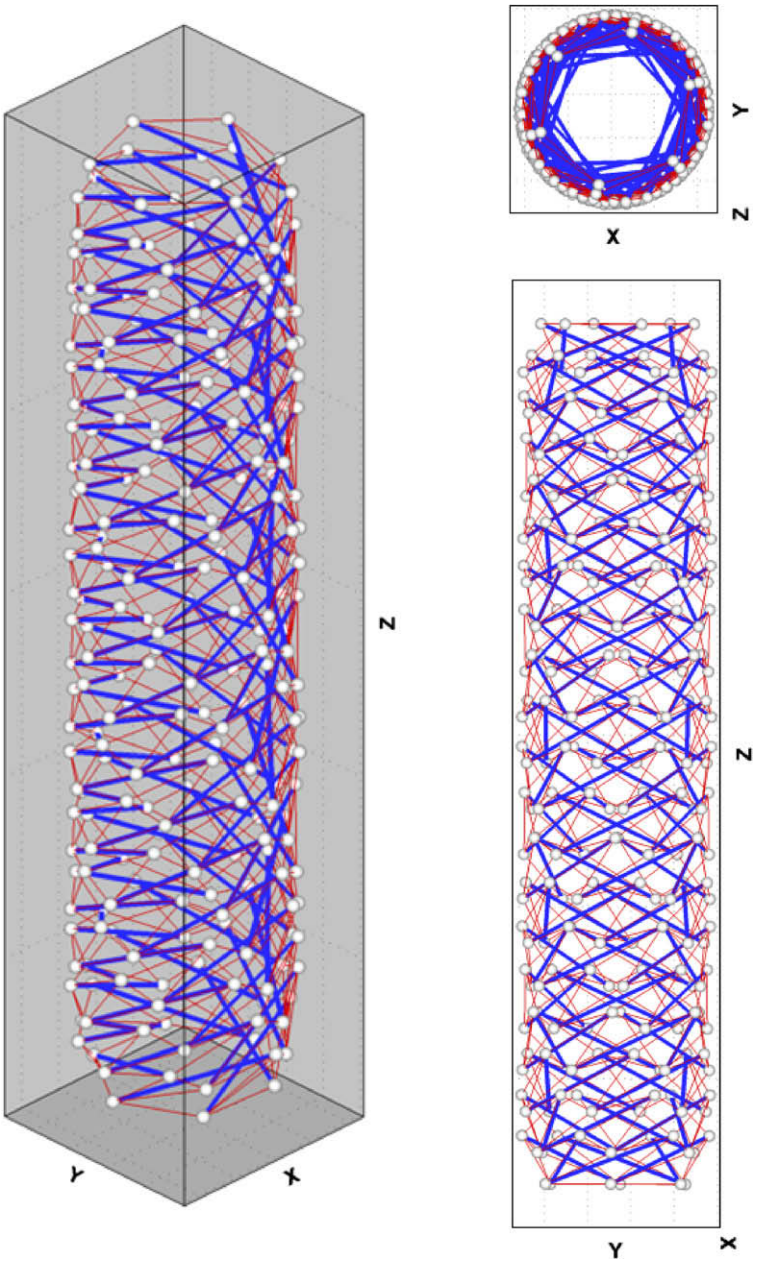

Fig. 7. Three orthographic views of a tensegrity tower of 20 stages.

only trial configurations with lower energy are accepted during iteration, the MCFF method is somewhat slower than the dynamic relaxation method for small scale problems. Nevertheless, it is still fast for most applications. For example, for a structure of less than 20 bars with a randomly selected initial configuration, the computation only takes a few seconds. Due to the stochastic approach employed in MCFF, the computational time is not really deterministic and can vary in a certain range even for repeated simulations of the same structure with the same initial configuration. For large scale problems, we have tested this new form-finding method for structures with thousands of bars, and found that the calculations can be typically completed in a few hours on a PC. Parallel computation can further increase the computational efficiency of MCFF.

4.2. Spherical tensegrity

As the second example, we consider spherical tensegrity structures in which all nodes lie on a spherical surface.

Truncated tetrahedral tensegrity is the simplest type of spherical tensegrity. Fig. 8(a) illustrates a regular tetrahedron and its truncated form. The form-finding result of a truncated tetrahedral tensegrity from the MCFF procedure is shown in Fig. 8(b). The strings of the truncated tetrahedral tensegrity have the same topology as the edges of the corresponding polyhedron. There are 12 truncating-edge strings and 6 vertical strings. We use q_t and q_v to denote the force densities (Linkwitz and Schek, 1971) in the truncating-edge strings and vertical strings, respectively. The structure has 6 bars and their force density is denoted by q_b.

Setting $q_t = 1$, we can obtain the relation between q_b and q_v under various combinations of original element lengths. The calculated results from the MCFF procedure, as plotted in Fig. 9, show good agreement with the corresponding analytical solutions (Tibert and Pellegrino, 2003; Pandia Raj and Guest, 2006).

For regular truncated dodecahedral and icosahedral tensegrity structures, the relations between the force densities q_b and q_v calculated from the MCFF procedure are shown in Figs. 10 and 11.

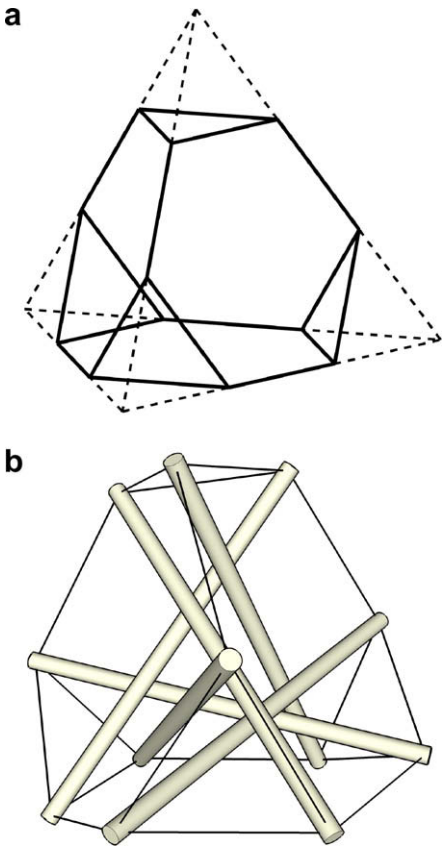

Fig. 8. (a) Truncated tetrahedron and (b) truncated tetrahedral tensegrity.

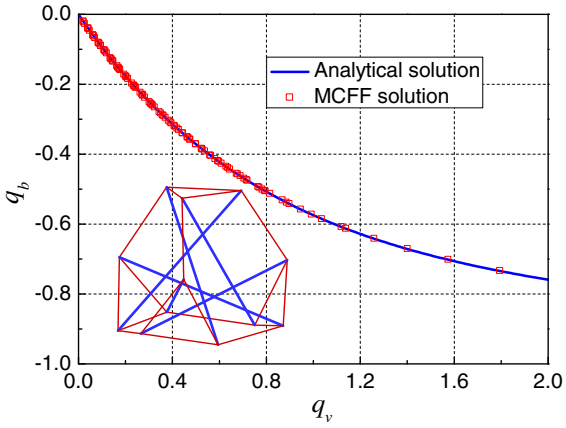

Fig. 9. Comparison between the results of q_b versus q_v for a truncated tetrahedral tensegrity calculated from the MCFF method (red squares) and the corresponding analytical solution (blue curve). (For interpretation of references to color the reader is referred to the web version of this article.)

Again, the results are found in good agreement with analytical solutions derived by Murakami and Nishimura (2001).

As another sample of spherical tensegrity, Fig. 12(a) shows an "expandable octahedron" (Tibert and Pellegrino, 2003) tensegrity consisting of 6 bars and 24 strings. We set the length of each bar as l_{0b} and that of each string as l_{0s}. All elements are assumed to have unit stiffness. The MCFF procedure is performed for various combinations of l_{0b} and l_{0s}. Let q_b and q_s denote the force densities, and l_b and l_s the lengths of the bars and the strings in the stable configuration of the tensegrity, respectively. We find that, regardless of the initial values of l_{0b} and l_{0s}, the force density ratio q_b/q_s is

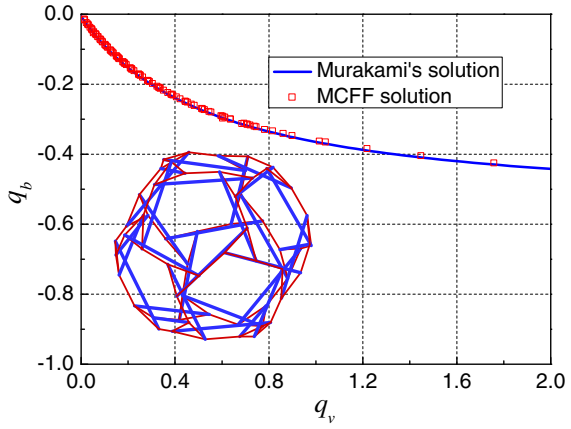

Fig. 10. Comparison between the results of q_b versus q_v for a truncated dodecahedral tensegrity obtained by the MCFF method (red squares) and the analytical solution of Murakami and Nishimura (2001) (blue curve). (For interpretation of references to color the reader is referred to the web version of this article.)

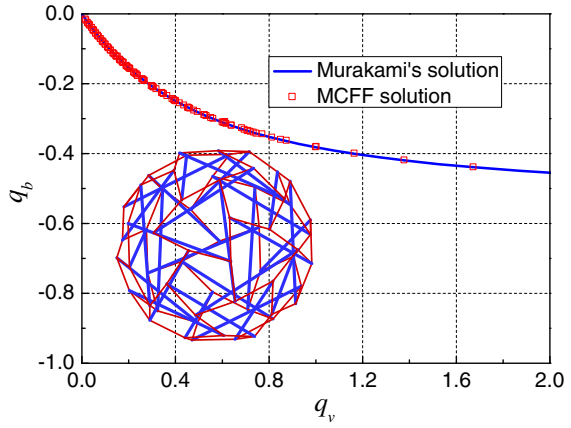

Fig. 11. Comparison of the result of q_b versus q_v for a truncated icosahedral tensegrity obtained by the MCFF method (red squares) and the analytical solution of Murakami and Nishimura, 2001 (blue curve). (For interpretation of references to color the reader is referred to the web version of this article.)

always equal to -1.500 and the length ratio l_b/l_s always equal to 1.633. These results are in perfect agreement with the numerical results (Estrada et al., 2006) and the corresponding analytical solutions $q_b/q_s = -3/2$ and $l_b/l_s = 2\sqrt{6}/3$ (Tibert and Pellegrino, 2003; Coughlin and Stamenovic, 1997).

In addition to the "expandable octahedron" configuration, we also found another equilibrium configuration from the same input file, as shown in Fig. 12(b). This configuration resembles a frustum, with the top face similar to the prismatic tensegrity structure $D_6^{3,3}$ (Zhang et al., 2009). This configuration is unstable even though all nodal forces are zero, with the smallest eigenvalue of its stiffness matrix being negative. After a few iteration steps, this intermediate form is replaced by the stable structure shown in Fig. 12(a). Here, it might be of interest to mention a conjecture by Volokh (2003): "*A tensegrity structure with all tensioned cables and compressed struts is always stable independently of its topology, geometry and specific magnitudes of member forces*". The structure in Fig. 12(b) is a counterexample of this incorrect conjecture. Another simple counterexample is given in Fig. 13, which satisfies all the conditions required in the conjecture but is unstable.

4.3. Irregular tensegrity structures

Form-finding problems of irregular tensegrities are generally very difficult to be solved analytically. The following examples

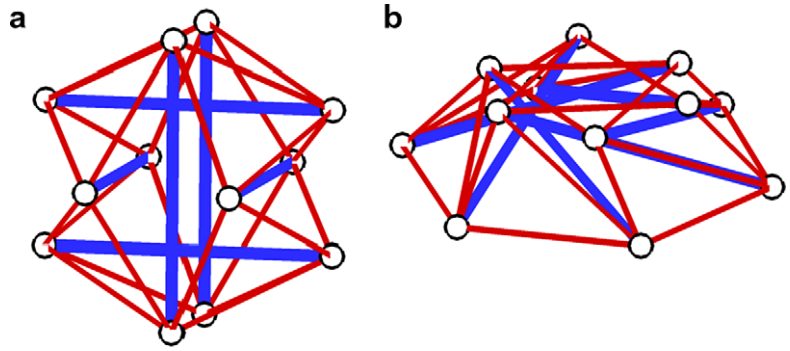

Fig. 12. (a) "Expandable octahedron" tensegrity structure calculated by the MCFF method and (b) an unstable equilibrium configuration obtained from the same initial configuration.

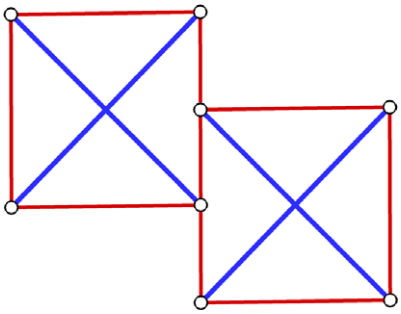

Fig. 13. A simple example showing that Volokh's 2003 conjecture about the stability of tensegrity structures is incorrect.

are used to demonstrate the applicability of the MCFF method for such structures.

Firstly, we consider two models having the same topology as a cylindrical tensegrity with $v = 50$ and $a = 1$. The length of strings on the top and bottom of the tensegrity is set to be 0.06, and the length of other strings is taken as 1.40. The stiffness of all elements is taken to be unity. In the first case, the original lengths of the bars constitute an arithmetic progression from 1.50 to 1.99 with a step difference of 0.01. The equilibrium configuration determined by the MCFF procedure is given in Fig. 14(a). In the second case, the original lengths of the bars are randomly selected with a uniform distribution between 1.00 and 2.00. The form-finding result is shown in Fig. 14(b).

Our simulations show that for the same input file of a truncated icosahedral tensegrity structure, the MCFF process sometimes leads to an irregular and stable configuration, as shown in Fig. 15. This means that for the same topology and properties of elements, there may exist multiple stable states. This result complies with that in Defossez (2003). The existence of multiple stable states without changing the resting lengths of elements provides clues to design novel deployable or foldable structures. This is an interesting issue and deserves further research.

Finally, we use the polyhedral truncation scheme to construct a more irregular tensegrity structure, as shown in Fig. 16. This structure has 69 bars, and the original length of bars and strings are set to be 10 and 3, respectively. More examples of using MCFF to find irregular tensegrity forms based on elementary cells consisting of only one bar can be found in Li et al. (2010).

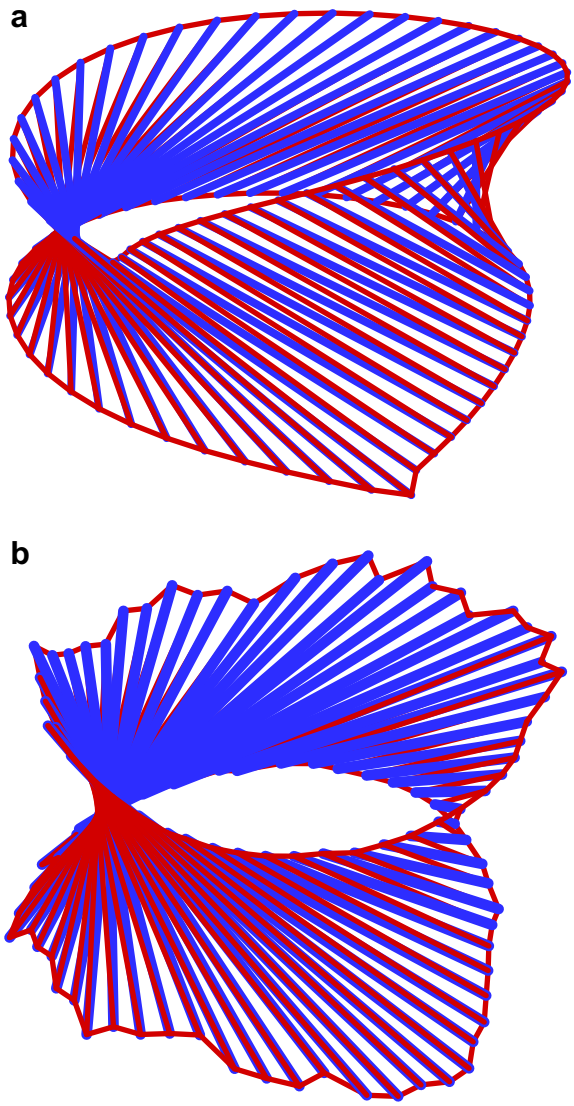

Fig. 14. Irregular cylindrical tensegrity structures calculated by the MCFF method.

5. Conclusions

We have developed a Monte Carlo-based form-finding (MCFF) method for large scale regular and irregular tensegrity structures. In this method, a stochastic process is employed to find equilibrium tensegrity forms. The MCFF procedure is easy to implement and only involves simple algebraic operations. It has been demonstrated that the proposed method can find tensegrity forms without prior knowledge on the nodal coordinates. The MCFF method can treat not only symmetric but also irregular tensegrity struc-

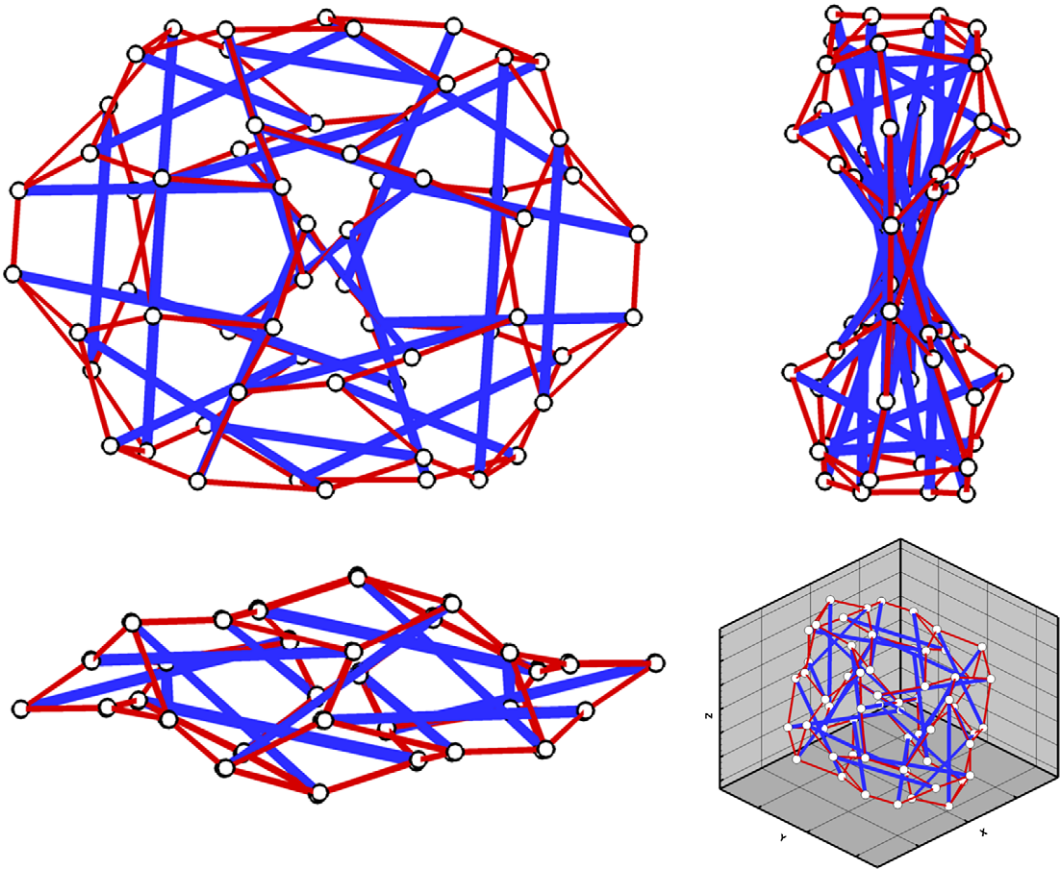

Fig. 15. An irregular but stable tensegrity structure with 30 bars and 90 strings.

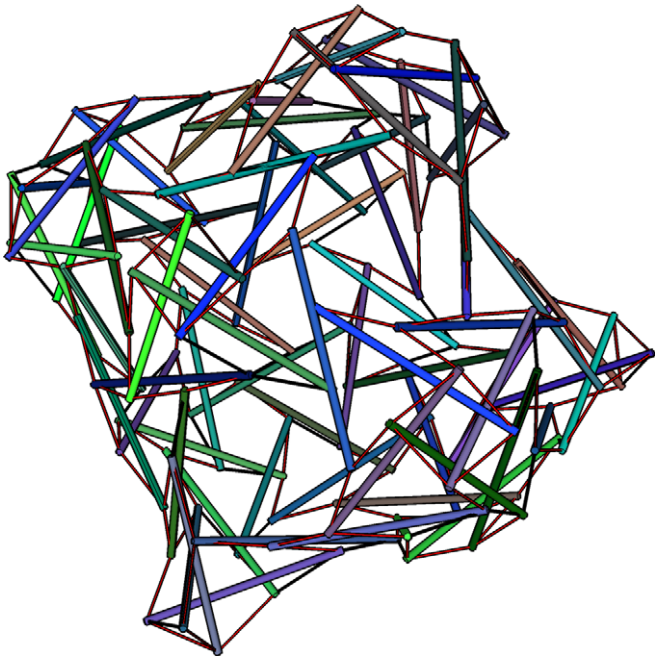

Fig. 16. Form-finding result of a fully irregular tensegrity structure.

tures at relatively large scales. A number of illustrative examples have been given to demonstrate the method. Finally, we point out that the present method can also be applied to tensegrity structures subjected to conservative force fields and/or displacement constraints.

Acknowledgments

Financial support from the National Natural Science Foundation of China (Grant Nos. 10525210 and 10732050) and 973 Project (2010CB631005) is acknowledged.

References

Calladine, C.R., 1978. Buckminster Fuller's tensegrity structures and Clerk Maxwell's rules for the construction of stiff frames. International Journal of Solids and Structures 14 (1), 161–172.
Connelly, R., 1993. Rigidity. In: Gruber, P., Wills, J. (Eds.), Handbook of Convex Geometry. Elsevier Publishers Ltd, pp. 223–271.
Connelly, R., Back, A., 1998. Mathematics and tensegrity. American Scientist 86 (2), 142–151.
Connelly, R., Terrell, M., 1995. Globally rigid symmetric tensegrities. Structural Topology (21), 9–81.
Coughlin, M.F., Stamenovic, D., 1997. A tensegrity structure with buckling compression elements: application to cell mechanics. Journal of Applied Mechanics 64 (3), 480–486.
Defossez, M., 2003. Shape memory effect in tensegrity structures. Mechanics Research Communications 30 (4), 311–316.
Ehara, S., Kanno, Y., 2010. Topology design of tensegrity structures via mixed integer programming. International Journal of Solids and Structures 47 (6), 571–579.
Estrada, G.G., Bungartz, H.J., Mohrdieck, C., 2006. Numerical form-finding of tensegrity structures. International Journal of Solids and Structures 43 (22–23), 6855–6868.
Feng, X.Q., Li, Y., Cao, Y.P., Yu, S.W., Gu, Y.T., in press. Design methods of rhombic tensegrity structures. Acta Mechanica Sinica.
Fu, F., 2005. Structural behavior and design methods of tensegrity domes. Journal of Constructional Steel Research 61 (1), 23–35.
Hanaor, A., 1988. Prestressed pin-jointed structures – flexibility analysis and prestress design. Computers and Structures 28 (6), 757–769.
Ingber, D.E., 1993. Cellular tensegrity: defining new rules of biological design that govern the cytoskeleton. Journal of Cell Science 104 (3), 613–627.
Ingber, D., 1997. Tensegrity: the architectural basis of cellular mechanotransduction. Annual Review of Physiology 59, 575–599.

Juan, S.H., Mirats Tur, J.M., 2008. Tensegrity frameworks: static analysis review. Mechanism and Machine Theory 43 (7), 859–881.
Kalos, M.H., Whitlock, P.A., 1986. Monte Carlo Methods. Wiley-Interscience.
Kenner, H., 2003. Geodesic Math and How to Use It. University of California Press, Berkeley, California.
Li, Y., Feng, X.Q., Cao, Y.P., Gao, H., 2010. Constructing tensegrity structures form one-bar elementary cells. Proceedings of the Royal Society A 466, 45–61.
Linkwitz, K., Schek, H.J., 1971. Einige bemerkungen zur berechnung von vorgespannten seilnetzkonstruktionen. Ingenieur Archiv 40 (3), 145–158.
Luo, H., Bewley, T.R., Smith, R.C., 2005. Accurate simulation of near-wall turbulence over a compliant tensegrity fabric. In: Smart Structures and Materials 2005: Modeling, Signal Processing, and Control, vol. 5757, SPIE, San Diego, CA, USA, pp. 184–197.
Masic, M., Skelton, R.E., Gill, P.E., 2005. Algebraic tensegrity form-finding. International Journal of Solids and Structures 42 (16–17), 4833–4858.
Masic, M., Skelton, R.E., Gill, P.E., 2006. Optimization of tensegrity structures. International Journal of Solids and Structures 43 (16), 4687–4703.
Metropolis, N., Ulam, S., 1949. The Monte Carlo method. Journal of the American Statistical Association 44 (247), 335–341. pMID: 18139350.
Metropolis, N., Rosenbluth, A.W., Rosenbluth, M.N., Teller, A.H., Teller, E., 1953. Equation of state calculations by fast computing machines. Journal of Chemical Physics 21 (6), 1087–1092.
Motro, R., 1984. Forms and forces in tensegrity systems. In: Proceedings of the Third International Conference on Space Structures. Elsevier, Amsterdam.
Murakami, H., Nishimura, Y., 2001. Initial shape finding and modal analyses of cyclic right-cylindrical tensegrity modules. Computers and Structures 79, 891–917.
Murakami, H., Nishimura, Y., 2001. Static and dynamic characterization of regular truncated icosahedral and dodecahedral tensegrity modules. International Journal of Solids and Structures 38 (50–51), 9359–9381.
Pagitz, M., Mirats Tur, J.M., 2009. Finite element based form-finding algorithm for tensegrity structures. International Journal of Solids and Structures 46 (17), 3235–3240.
Pandia Raj, R., Guest, S., 2006. Using symmetry for tensegrity form-finding, in: International Association for Shell and Spatial Structures, Beijing, China.
Paul, C., Lipson, H., Cuevas, F.J.V., 2005. Evolutionary form-finding of tensegrity structures. In: Proceedings of the 2005 Conference on Genetic and Evolutionary Computation. ACM, Washington, USA.
Pellegrino, S., Calladine, C.R., 1986. Matrix analysis of statically and kinematically indetermined frameworks. International Journal of Solids and Structures 22 (4), 409–428.
Pirentis, A.P., Lazopoulos, K.A., 2010. On the singularities of a constrained (incompressible-like) tensegrity-cytoskeleton model under equitriaxial loading. International Journal of Solids and Structures 47 (6), 759–767.
Rieffel, J., Valero-Cuevas, F., Lipson, H., 2009. Automated discovery and optimization of large irregular tensegrity structures. Computers and Structures 87, 368–379.
Schek, H.J., 1974. The force density method for form finding and computation of general networks. Journal of Computer Methods in Applied Mechanics and Engineering 3, 115–134.
Snelson, K.D., 1965. Continuous tension, discontinuous compression structures. United States Patent 3169611.
Spall, J.C., 2003. Introduction to Stochastic Search and Optimization. Wiley-Interscience.
Sultan, C., 2009. Tensegrity: 60 years of art, science and engineering. Advances in Applied Mechanics 43, 69–145.
Sultan, C., Corless, M., Skelton, R.E., 2001. The prestressability problem of tensegrity structures: some analytical solutions. International Journal of Solids and Structures 38 (30–31), 5223–5252.
Tibert, A.G., Pellegrino, S., 2002. Deployable tensegrity reflectors for small satellites. Journal of Spacecraft and Rockets 39 (5), 701–709.
Tibert, A.G., Pellegrino, S., 2003. Review of form-finding methods for tensegrity structures. International Journal of Space Structures 18, 209–223.
Vassart, N., Motro, R., 1999. Multiparametered formfinding method: application to tensegrity systems. International Journal of Space Structures 14, 147–154.
Volokh, K.Y., 2003. Stability conjecture in the theory of tensegrity structures. International Journal of Structural Stability and Dynamics 3 (1), 1–16.
Williamson, D., Skelton, R.E., Han, J., 2003. Equilibrium conditions of a tensegrity structure. International Journal of Solids and Structures 40 (23), 6347–6367.
Zhang, J., Ohsaki, M., 2005. Form-finding of self-stressed structures by an extended force density method. Journal of the International Association for Shell and Spatial Structures 46 (3), 159–166.
Zhang, J.Y., Ohsaki, M., 2006. Form-finding of tensegrity structures subjected to geometrical constraints. International Journal of Space Structures 21, 183–196.
Zhang, J.Y., Guest, S.D., Ohsaki, M., 2009. Symmetric prismatic tensegrity structures: Part I. Configuration and stability. International Journal of Solids and Structures 46, 1–14.